ELSEVIER

Inorganica Chimica Acta 223 (1994) 145–149

Inorganica Chimica Acta

Note

Synthesis and X-ray analysis of the dirhodium(II,II) carboxylate complex $Rh_2(O_2CCH_3)_4(formH)_2$ (formH = *N,N'*-di-*p*-tolylformamidine)

Francesco Nicolò, Giuseppe Bruno, Sandra Lo Schiavo, Maria S. Sinicropi, Pasquale Piraino*

Dipartimento di Chimica Inorganica, Analitica e Struttura Molecolare, Università di Messina, 98166 Vill. S. Agata, Messina, Italy

Received by Editor 29 November 1993; received by Publisher 7 March 1994

Abstract

The tetrakisacetate dirhodium(II,II) complex reacts with *N,N'*-di-*p*-tolylformamidine (formH) giving the bisadduct $Rh_2(O_2CCH_3)_4(formH)_2$. The complex crystallizes in the monoclinic space group $P2_1/c$, with $a = 11.638(2)$, $b = 12.464(3)$, $c = 17.303(4)$ Å, $\beta = 98.09(2)°$, $V = 2484.9(9)$ Å^3, $Z = 2$ and $D_{calc} = 1.506$ g cm^{-3}. The structure reveals that bond lengths and angles within the $Rh_2(O_2CCH_3)_4$ fragment are in the range quoted for similar complexes. It also reveals that the two formamidines are axially bonded to the dirhodium core through the imino nitrogen. The N–C–N formamidine planes are rotated by 100.00(4)° with respect to the equatorial planes of the two rhodium atoms, leading to several hydrogen-bonding interactions. The ^{1}H NMR spectrum exhibits features that do not correspond to the solid-state geometry. It shows in fact only one signal for the methyl groups of the formamidine, suggesting that the title complex is subject to a fluxional process that involves fast exchange of the coordination sites, amino and imino, of formamidine.

Keywords: Crystal structures; Rhodium complexes; Carboxylate complexes; Dinuclear complexes

1. Introduction

Some years ago we reported the synthesis and electrochemical behaviour of two interesting Rh_2^{4+} complexes, namely $Rh_2(form)_2(O_2CCF_3)_2(H_2O)_2$ (**I**) and $Rh_2(form)_4$ (**II**) (form = *N,N'*-di-*p*-tolylformamidinate anion), whose schematic structures are reported in Fig. 1 [1,2]. Complex **I** is a very reactive species, exhibiting equatorial reactivity in addition to the usual axial reactivity [3,4]. But the presence of two strong electron-withdrawing trifluoroacetate groups makes this species less easily oxidizable than the tetrakisformamidinate derivative. On the other hand, species **II** is inert toward equatorial substitution and shows only poor axial reactivity for steric reasons. However, the presence of four good σ-donor groups facilitates the thermodynamic access to species containing the Rh_2^{5+} core [5].

The different redox properties of the two complexes are also reflected by their oxidation potentials (0.76 and 0.25 V versus SCE, respectively) and by their reactivity with electron-acceptor molecules such as TCNE (tetracyanoethylene) and TCQM (tetracyanoquinodimethane). Complex **I** reacts by simple axial coordination, while complex **II** reacts via a redox reaction [6].

With the aim of accomplishing, using the same molecule, both substitutional and redox processes, we postulated the substitution in complex **I** of the trifluoroacetate groups by the less electron-withdrawing acetates. It is worth mentioning that while the $Rh_2(O_2CCH_3)_4$ complex undergoes a mono-electron oxidation at ~1 V [7], the corresponding fluorocarboxylate is not oxidized in the potential range of any of the solvents utilized. This paper reports the experimental details used for the synthesis of the $Rh_2(form)_2(O_2CCH_3)_2$

*Corresponding author.

SSDI 0020-1693(94)03962-N

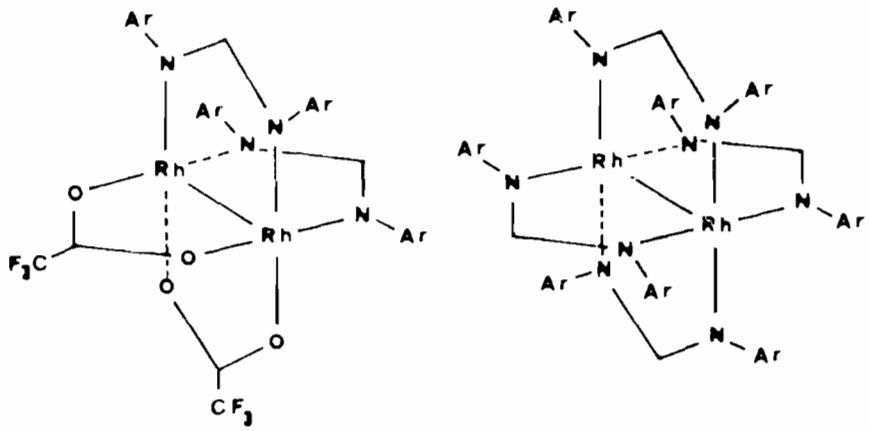

I II

Fig. 1. Schematic structure of $Rh_2(form)_2(O_2CCF_3)_2(H_2O)_2$ (**I**) and $Rh_2(form)_4$ (**II**) (form = *N,N'*-di-*p*-tolylformamidinate anion).

complex and the synthesis and X-ray crystal structure of the complex $Rh_2(O_2CCH_3)_4(formH)_2$.

2. Experimental

N,N'-Di-*p*-tolylformamidine was synthesized according to a literature procedure [8]. Other reagents and solvents were used as received. IR spectra were recorded on a Perkin-Elmer FT 43 instrument. ^1H NMR spectra were recorded using a Bruker AMX 300 spectrometer.

2.1. Synthesis of $Rh_2(O_2CCH_3)_4(formH)_2$ (1)

$Rh_2(O_2CCH_3)_4(formH)_2$ (**1**) was synthesized as follows. 120 mg (0.27 mmol) of $Rh_2(O_2CCH_3)_4$ dissolved in $CHCl_3$ were allowed to react with *N,N'*-di-*p*-tolylformamidine (121.6 mg, 0.54 mmol). After 2 h the colour of the solution was red–violet. The solution was filtered and dried in vacuo, leading to a red–violet solid, which was crystallized from $CHCl_3$–heptane (yield 85%). *Anal.* Found: C, 46.2; H, 4.5; N, 5.68. Calc. for $C_{39}H_{45}O_8N_4Cl_3Rh_2$: C, 46.38; H, 4.49; N, 5.54. ^1H NMR spectrum ($CDCl_3$, r.t.): δ 1.83 (s, 12H), 2.31 (s, 12H), 8.67 (s, 2H).

2.2. X-ray data collection and structure refinement

Suitable violet crystals were obtained by slow evaporation of the solvent from a $CHCl_3$–heptane solution. Diffraction data were collected at room temperature with a Siemens R3m/v automatic four-circle diffractometer using graphite-monochromated Mo Kα radiation. Cell parameters were obtained from 25 accurately centered reflections with 2θ in the range 14–28°. The compound crystallizes in the monoclinic space group $P2_1/c$, with $a = 11.638(2)$, $b = 12.464(3)$, $c = 17.303(4)$ Å, $\beta = 98.09(2)°$, $V = 2484.9(9)$ Å^3, $Z = 2$ and $D_{calc} = 1.506$ g cm^{-3}. Further information on crystallographic data collection and refinement of the structure determination are reported in Table 1.

Table 1
Crystal and refinement data for complex **1**

Formula	$C_{39}H_{45}Cl_3N_4O_8Rh_2$
Formula weight	1127.4
Crystal system	monoclinic
Space group	$P2_1/c$
a (Å)	11.638(2)
b (Å)	12.464(3)
c (Å)	17.303(4)
β (°)	98.09(2)
V (Å^3)	2486.0(17)
Z	2
ρ_{calc} (g cm^{-3})	1.506
Crystal size (mm)	0.28×0.32×0.41
Orientation reflections no., range (2θ)	25, $15 < 2\theta < 28$
T (°C)	23
μ (cm^{-1})	10.36
Radiation, λ (Å)	Mo Kα, 0.71073
Monochromator	graphite crystal
Scan type	ω–2θ
Scan speed (°/min)	2.49 to 5.01 in ω
Scan range (°)	1.2° plus Kα separation
Standard reflections	3 measured after every 140 min
Data limits	$3 < 2\theta < 50$
No. data collected	5548
Observed data	2190 ($F \geq 7\sigma(F)$)
Absorption correction	semi-empirical
No. parameters refined	298
R[a]	0.021
R_w[b]	0.0301
Quality-of-fit indicator[c]	0.941
Weighting scheme	$w = 1/(\sigma^2(F_o) + 0.0344F_o^2)$
Largest peak (e Å^{-3})	0.69

[a] $R = [\Sigma||F_o| - |F_c||]/\Sigma|F_o|$.
[b] $R_w = [\Sigma w[\Sigma(|F_o| - |F_c|)^2/\Sigma w|F_o|^2]^{1/2}$, $w = n/(\sigma^2(F_o))$.
[c] Quality-of-fit = $[\Sigma w(|F_o| - |F_c|)^2/(N_{obs} - N_{param})]^{1/2}$.

5548 reflections were collected by the variable-speed ω–2θ scan method up to a 2θ value of 50°, with index ranges $-1 \leq h \leq 13$, $-18 \leq k \leq 18$, $-19 \leq l \leq 19$. From the corresponding 4411 unique reflections ($R_{int} = 4.5\%$), 2190 were considered observed ($F_o \geq 7\sigma(F_o)$) for the refinement of the structure model. The intensities of three standard reflections, monitored after every 97 measurements, decrease to about 10% of the corresponding starting values.

The diffraction data were processed with the learnt-profile procedure [9] and then corrected for decay and Lorentz–polarization effects. Absorption correction was applied by fitting a pseudo-ellipsoid to the azimuthal scan data of 16 suitable reflections with high χ angles [10]. The structure was solved by standard Patterson methods and subsequently completed by a combination of least-squares technique and Fourier syntheses. All non-hydrogen atoms were refined anisotropically. Hydrogen atoms were added at calculated positions and included in the structure factor calculations with a common thermal parameter ($U = 0.06$ Å^2). The structure model was refined by full-matrix least-squares technique, minimizing the function $\Sigma w(F_o^2 - F_c^2)^2$, converging to $R = \Sigma|F_o - F_c|/\Sigma F_o = 0.021$ and $R_w = [\Sigma w(F_o^2 - F_c^2)^2 / \Sigma w - (F_o^2)^2]^{1/2} = 0.0301$, with the final weighting scheme $w = [\sigma^2(F_o^2) + 0.0344F_c^2]$. The last difference map showed the largest electron density residuals (max. and min. range ± 0.69 e Å^{-3}) at about 1 Å from the rhodium atom. Other important residuals were obtained around the chloroform molecules owing to a rotational disorder of their Cl atoms. Neutral-atom scattering factors and anomalous dispersion corrections were taken into account [11].

Data reduction and structure solutions and drawings were performed using the SHELXTL-PLUS package [12], while structure refinement and final geometrical calculations were carried out with the SHELXL-93 [13] and PARST programs [14], respectively, on a DEC Micro Vax/3400 computer.

3. Results and discussion

One of the synthetic procedures adopted for the synthesis of the complex $Rh_2(form)_2(O_2CCH_3)_2$ required, as the first step, the synthesis of the complex $Rh_2(O_2CCH_3)_4(formH)_2$ (formH = *N*,*N*′-di-*p*-tolylformamidine). Although neutral formamidine derivatives are rare, this species was easily synthesized by reacting the complex $Rh_2(O_2CCH_3)_4$ with *N*,*N*′-di-*p*-tolylformamidine, at a molar ratio of 1:2. The red–violet complex obtained was characterized by spectroscopic measurements and X-ray analysis. The monodentate bonding mode of formH was inferred from the solid-state IR data, which show ν_{asym}(NCN) at 1651 cm^{-1}, very close to the value exhibited by monocoordinated or uncoordinated formH. The absorption at 3232 cm^{-1} is also indicative of N–H stretching. The ^{1}H NMR spectrum, however, exhibits features that do not correspond to the solid-state geometry (see below), which indicates that the azotate ligands are bonded to the metal through the less basic imino nitrogen. This would imply non-equivalence of the tolyl groups. But the complex shows, in the methyl region, two signals at 1.83 and 2.31 ppm (intensity ratio 1:1), attributed to the methyl groups of the carboxylate and formamidinate groups, respectively. Furthermore, the AB spin system of the aromatic protons appears as a single set of signals centered at 6.98 ppm. The CH imine protons appear as a broad singlet at 8.67 ppm, while the NH signal is not apparent. These data suggest that the title complex is subject to a process that involves fast exchange of the coordination sites, amino and imino, of the formamidine. This exchange is possibly the result of the well-known ability of dirhodium(II,II) complexes to undergo dissociation of the axial ligands. ^{1}H NMR experiments show that, behind the coalescence temperature, coordinated formamidine rapidly exchanges with the free ligand, while the spectra of the pure complex at various concentrations allow us to exclude any bimolecular complex–complex interaction. The above-described dynamic behaviour of formH is not unprecedented. Vrieze and co-workers reported that the complex $[Pd\{C_6H_3(CH_2NMe_2)_2\text{-}2,6\}(formH)]X$ (formH = *N*,*N*′-di-*p*-tolylformamidine; $X = BF_4$, CF_3SO_3) [15], bearing a neutral monodentate formamidine, is subject at high temperature to a fluxional process arising from an anion-assisted formH dissociation [8].

The second step of the synthesis involved deprotonation of the amino nitrogen and conversion of the formamidine to a formamidinate derivative, with consequent elimination of two acetate groups from the lantern structure. However, all attempts were unsuccessful. In fact, reaction of the title complex in high-boiling solvents or under the conditions used for formation of the formamidinate anion, namely in the presence of bases, produced after one day only a greenish product corresponding to the empirical formula $Rh(O_2CCH_3)$, which we were unable to characterize.

The second procedure adopted involved the chemical oxidation of the complex $[C_8H_{12}Rh(form)]_2$ with CH_3COOAg. This synthetic procedure has successfully been used to synthesize complex **I** using CF_3COOAg [1]. Unfortunately, this route also failed.

3.1. Crystal structure of $[Rh_2(O_2CCH_3)_4(formH)_2]CHCl_3$

Fig. 2 shows the ORTEP drawing of the complex together with the atomic number scheme. Selected bond distances and angles are given in Table 2. Final positional parameters are reported in Table 3. The molecule,

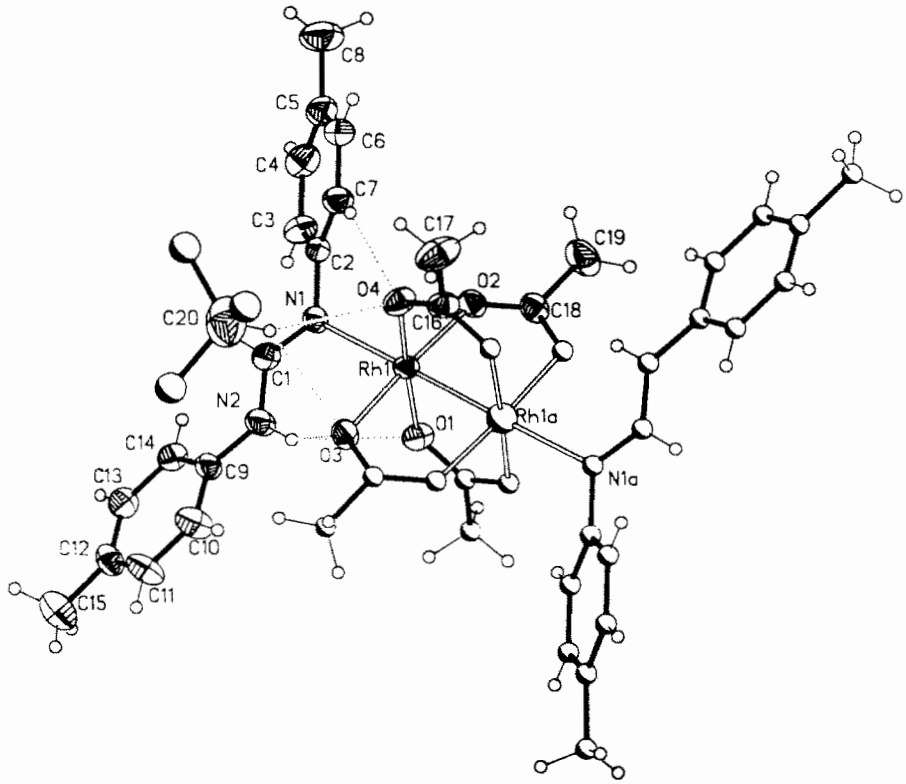

Fig. 2. An ORTEP view of $Rh_2(O_2CCH_3)_4(formH)_2$ (**1**) showing 40% probability thermal ellipsoids.

Table 2
Selected bond distances (Å) and angles (°)

Bond distances			
Rh(1)–Rh(1)′	2.412(1)		
Rh(1)–N(1)	2.309(4)	N(2)–C(9)	1.407(7)
Rh(1)–O(1)	2.037(3)	O(2)–C(18)	1.251(6)
Rh(1)–O(2)	2.034(4)	O(4)–C(16)	1.268(6)
Rh(1)–O(3)	2.043(3)	C(16)–C(17)	1.507(8)
Rh(1)–O(4)	2.046(4)	C(18)–C(19)	1.514(8)
N(1)–C(1)	1.285(7)	C(20)–Cl(1)	1.62(1)
N(1)–C(2)	1.436(6)	C(20)–Cl(2)	1.74(1)
C(1)–N(2)	1.334(7)	C(20)–Cl(3)	1.71(1)
Bond angles			
O(3)–Rh(1)–O(4)	89.5(1)	C(1)–N(1)–C(2)	117.2(4)
O(2)–Rh(1)–O(4)	90.7(1)	N(1)–C(1)–N(2)	122.6(5)
O(2)–Rh(1)–O(3)	175.6(1)	C(1)–N(2)–C(9)	127.0(4)
O(1)–Rh(1)–O(4)	175.2(1)	N(1)–C(2)–C(7)	119.1(4)
O(1)–Rh(1)–O(3)	89.1(1)	N(1)–C(2)–C(3)	122.2(4)
O(1)–Rh(1)–O(2)	90.3(1)	N(2)–C(9)–C(14)	123.3(5)
N(1)–Rh(1)–O(4)	94.8(1)	N(2)–C(9)–C(10)	118.1(5)
N(1)–Rh(1)–O(3)	93.6(1)	Rh(1)–O(2)–C(18)	119.0(3)
N(1)–Rh(1)–O(2)	90.7(1)	Rh(1)–O(4)–C(16)	119.3(3)
N(1)–Rh(1)–O(1)	89.8(1)	O(4)–C(16)–C(17)	117.2(5)
Rh(1)–N(1)–C(2)	120.5(3)	O(2)–C(18)–C(19)	117.8(5)
Rh(1)–N(1)–C(1)	121.4(3)		

which consists of discrete binuclear $Rh_2(O_2CCH_3)_4$-$(formH)_2$ units and one chloroform crystallization molecule, is a dimer lying on a crystallographic inversion centre, with each rhodium atom exhibiting distorted octahedral coordination. Four carboxylate ligands are bridged across the Rh–Rh core to give the usual 'lantern' dinuclear structure. Two mono-ligated formamidine groups, located at the axial positions, complete the coordination of the metal centres.

The rhodium–rhodium bond length of 2.412(1) Å is equal (within the e.s.d.s) to that found in $[Rh_2(O_2CCH_3)_4(dptH)_2]$ (dptH = diphenyltriazene) [16] and is in good agreement with the values previously reported for analogous complexes. The neutral formamidine ligands are bonded to the axial sites via the imino N1 (N1′) atoms. Such a bonding mode for the neutral ligand was first encountered in $[Pt\{C_6H_3$-(CH_2NMe_2)-2,6$\}(dptfH)][CF_3SO_3]$ [16]. The Rh–N1 bond distance (2.309(4) Å) as well as the Rh–Rh–N bond angle of 177.4(1)° are equal to those for the above-cited linear triazene complex and are similar to those found in other dinuclear rhodium(II) carboxylates containing amine or imino ligands coordinated at the axial coordination position [17]. The bond distances within the N–C–N formamidine skeleton (N1–C1, 1.285(7) Å) are outside the range quoted for N–C bonds of orders 2 and 1.

Although these values denote some degree of electronic delocalization, a greater multiple bond character for the N1–C1 fragment is apparent. Therefore the bonding description is consistent with an imino character for the N1 and N1′ atoms and an amino character for the N2 and N2′ atoms. The sum of the interbond angles around N1 (359.2(3)°) and N2 (358.7(5)°) as well as

Table 3
Fractional atomic coordinates ($\times 10^4$)

Atom	x	y	z
Rh(1)	914.1(4)	223.4(3)	385.5(2)
N(1)	2700(3)	586(3)	1100(2)
C(1)	3534(4)	986(4)	778(3)
N(2)	3392(4)	1324(4)	39(2)
C(2)	2978(4)	202(4)	1887(3)
C(3)	4013(4)	−305(4)	2148(3)
C(4)	4253(5)	−652(5)	2920(3)
C(5)	3465(6)	−497(4)	3442(3)
C(6)	2435(5)	−3(4)	3166(3)
C(7)	2180(5)	345(5)	2404(3)
C(8)	3746(6)	−844(6)	4290(3)
C(9)	4245(4)	1769(4)	−365(3)
C(10)	3891(5)	2444(5)	−978(3)
C(11)	4690(5)	2886(5)	−1409(3)
C(12)	5856(5)	2672(5)	−1232(3)
C(13)	6205(5)	2004(4)	−614(3)
C(14)	5424(4)	1540(4)	−184(3)
C(15)	6716(5)	3155(5)	−1707(4)
O(1)	1716(3)	−554(3)	−426(2)
O(2)	807(3)	−1176(3)	976(2)
O(3)	909(3)	1593(3)	−263(2)
O(4)	−16(3)	1001(3)	1134(2)
C(16)	−1115(5)	980(5)	1005(3)
C(17)	−1761(5)	1522(6)	1593(3)
C(18)	−66(5)	−1760(5)	805(3)
C(19)	−146(5)	−2771(5)	1279(3)
C(20)	1497(8)	3379(6)	1235(5)
Cl(1)	281(7)	3944(7)	1365(8)
Cl(2)	2477(5)	3306(5)	2153(3)
Cl(3)	2287(10)	3984(9)	592(4)
Cl(1′)	161(15)	3970(13)	709(7)
Cl(2′)	1414(18)	3663(11)	2105(6)
Cl(3′)	2503(14)	3860(16)	749(11)

the clear location of H2 on the N2 atom confirmed the above assumption. The *p*-tolyl substituents on N1 and N2 are twisted out of the N–C–N plane by 142.1(5)° and 154.4(4)°, respectively, in such a way that their interplane angle is 30.1(2)°. Furthermore, the N–C–N formamidine planes make an angle of 100.0(4)° with the equatorial rhodium planes. This geometry appears to be doubly advantageous, as it allows minimization of unfavourable steric interactions and, more importantly, the formation of two intermolecular hydrogen bonds between the amino hydrogen H2 and the acetate oxygen O3 (N2···O3 2.883(5) Å, H2···O3 2.122(5) Å, N2–H2–O3 147.2(5)°) and between the *o*-hydrogen H7 and the acetate oxygen O4 (C7···O4 3.232(5) Å, H7···O4 2.423(6) Å, C7–H7–O4 145.3(5)°). The rhodium–oxygen bond lengths fall, as usual, within a very narrow range (from 2.034(4) to 2.046(4) Å), the longest, Rh1–O3, associated with the strongest hydrogen bond, H2···O3. As can be seen from the O–Rh–Rh–O torsion angles, there is no significant twisting about the Rh–Rh bond. The chloroform molecule of crystallization is involved in weak intramolecular bifunctional hydrogen bonds (C20···O3 3.413(7) Å, H20···O3 2.614(3) Å, C20–H20–O3 138.8(5)°; C20···O4 3.440(7) Å, H20···O4 2.591(4) Å, C20–H20–O4 144.8(5)°), and consequently the chlorine atoms display the usual high librational motion.

The molecular packing is essentially due to van der Waals interactions as well as other weak intermolecular hydrogen bonds.

4. Supplementary material

Tables listing the atomic parameters of the hydrogen atoms, thermal parameters, complete bond distances and angles, and observed and calculated structure factors are available from the authors.

Acknowledgements

The authors thank the Ministero Università, Ricerca Scientifica and Tecnologia and the Italian Consiglio Nazionale delle Ricerche for financial support.

References

[1] P. Piraino, G. Bruno, G. Tresoldi, S. Lo Schiavo and P. Zanello, *Inorg. Chem., 26* (1987) 91.
[2] P. Piraino, G. Bruno, S. Lo Schiavo, F. Laschi and P. Zanello, *Inorg. Chem., 26* (1987) 2205.
[3] E. Rotondo, P. Piraino, B. Mann and G. Tresoldi, *Inorg. Chem., 28* (1989) 3070.
[4] E. Rotondo, G. Bruno, F. Nicolò, S. Lo Schiavo and P. Piraino, *Inorg. Chem., 30* (1991) 1195.
[5] G. Bruno, S. Lo Schiavo, G. Tresoldi, L. Valli and P. Piraino, *Inorg. Chim. Acta, 196* (1992) 131.
[6] F. Nicolò, G. Bruno, S. Lo Schiavo, M.S. Sinicropi and P. Piraino, work in progress.
[7] K. Das, K.M. Kadish and J.L. Bear, *Inorg. Chem., 17* (1978) 930.
[8] R.M. Roberts, *J. Am. Chem. Soc., 71* (1949) 3848.
[9] R. Diamond, *Acta Crystallogr., Sect. A, 27* (1969) 43.
[10] G. Kopfmann and R. Huber, *Acta Crystallogr., Sect. A, 24* (1968) 348.
[11] A.J.C. Wilson (ed.), *International Tables for X-ray Crystallography*, Kluwer, Dordrecht, 1992.
[12] *SHELXTL-PLUS*, Version 4.2, Siemens Analytical X-ray Instruments Inc., Madison, WI, 1991.
[13] (a) G.M. Sheldrich, *Acta Crystallogr., Sect. A, 46* (1990) 467; (b) G.M. Sheldrich, Z. Dauter, K.S. Wilson, H. Hope and L.C. Sieker, *Acta Crystallogr., Sect. D, 49* (1993) 18.
[14] M. Nardelli, *Comput. Chem., 7* (1983) 95 (version locally modified).
[15] D.M. Grove, G. van Koten, H.J.C. Ubbels, K. Vrieze, L.C. Niemann and C.H. Stam, *J. Chem. Soc., Dalton Trans.*, (1986) 717.
[16] N. Farrel, M.D. Vargas, Y.A. Mascarenhas and M.T. do P. Gambardella, *Inorg. Chem., 26* (1987) 1426.
[17] J.R. Rubin, T.P. Haromy and M. Sundaralingam, *Acta Crystallogr., Sect. C, 47* (1991) 1712.